Journal of Physics: Conference Series **420** (2013) 012074 doi:10.1088/1742-6596/420/1/012074

# Medium effects in direct reactions

**M Karakoc[(1,2)], and C Bertulani[(1)]**

[(1)]Department of Physics and Astronomy, Texas A&M University-Commerce, Commerce, Texas 75429-3011, USA
[(2)]Department of Physics, Akdeniz University, TR-07058 Antalya, Turkey

E-mail: mesut.karakoc@tamuc.edu

E-mail: carlos.bertulani@tamuc.edu

**Abstract.** We discuss medium corrections of the nucleon-nucleon (NN) cross sections and their influence on direct reactions at intermediate energies $\gtrsim$ 50 MeV/nucleon. The results obtained with free NN cross sections are compared with those obtained with a geometrical treatment of Pauli-blocking and Dirac-Bruecker methods. We show that medium corrections may lead to sizable modifications for collisions at intermediate energies and that they are more pronounced in reactions involving weakly bound nuclei.

## 1. Introduction

A carefully constructed optical potential is a crucial ingredient for the description of direct reactions, such as knockout reactions at intermediate and high energies [1] ($\gtrsim$ 50 MeV/nucleon). A microscopic method to deduce optical potentials is based on the construction of the potentials using an effective nucleon-nucleon (NN) interaction, or cross section (e.g. those of Ref. [2]). This technique is often used to construct the real part of an optical potential and with its imaginary part assumed rescaled in strength to better reproduce experimental data on elastic scattering, or total reaction cross sections. The real and imaginary parts of the potential can also be constructed independently as in Refs. [3, 4], where the procedure starts from a NN effective interaction with independent real and imaginary parts. It has also been shown that one can use nucleon-nucleon cross sections as the microscopic input [1], instead of nucleon-nucleon interactions. In this case, an effective treatment of Pauli-blocking on nucleon-nucleon scattering is needed, as it manifests through medium density dependence. In fact, it is well known that a proper numerical modeling of heavy-ion central collision dynamics requires to account for medium effects on the nucleon-nucleon cross sections [5]. The main goal of studies addressing these collisions is to learn more about the equation of state (EOS) through global collective variables.

Medium modifications of NN scattering have smaller effects in direct reactions since generally low nuclear densities are probed. Although, no comparison with experimental data was supplied, a first work on this effect in knockout reactions was presented in Ref. [6]. In this contribution, we report recent progress on studies of medium modifications in knockout reactions. We will report on medium effects in the NN cross section for the description of knockout reactions by means of (a) a geometrical treatment of Pauli-blocking and a (b) Dirac-Brueckner treatment. A comparison of our calculations to a large number of published experimental data is shown, and full results will be published else where [7]. The aim of this project is to obtain more

accurate spectroscopic factors that will lead to better understanding nuclear structure and to check and improve the credibility of the use of knockout reactions as an indirect methods for nuclear astrophysics.

## 2. Medium effects

### *2.1. Nucleon-nucleon cross sections*

In the literature, there are different fits to the free (total) nucleon-nucleon cross sections, such as those in Refs. [6, 8]. In this work, we have used the parametrization from the Ref. [6] which is obtained using the experimental data from Particle Data Group [9]. For practical reasons, the free nucleon-nucleon cross sections are separated in three energy intervals, by means of the expressions

$$\sigma_{pp} = \begin{cases} 19.6 + 4253/E - 375/\sqrt{E} + 3.86 \times 10^{-2} E \\ \text{(for } E < 280 \text{ MeV)} \\ \\ 32.7 - 5.52 \times 10^{-2} E + 3.53 \times 10^{-7} E^3 \\ -2.97 \times 10^{-10} E^4 \\ \text{(for 280 MeV} \leq E < 840 \text{ MeV)} \\ \\ 50.9 - 3.8 \times 10^{-3} E + 2.78 \times 10^{-7} E^2 \\ +1.92 \times 10^{-15} E^4 \\ \text{(for 840 MeV} \leq E \leq 5 \text{ GeV)} \end{cases} \quad (1)$$

for proton-proton collisions, and

$$\sigma_{np} = \begin{cases} 89.4 - 2025/\sqrt{E} + 19108/E - 43535/E^2 \\ \text{(for } E < 300 \text{ MeV)} \\ \\ 14.2 + 5436/E + 3.72 \times 10^{-5} E^2 - 7.55 \times 10^{-9} E^3 \\ \text{(for 300 MeV} \leq E < 700 \text{ MeV)} \\ \\ 33.9 + 6.1 \times 10^{-3} E - 1.55 \times 10^{-6} E^2 \\ +1.3 \times 10^{-10} E^3 \\ \text{(for 700 MeV} \leq E \leq 5 \text{ GeV)} \end{cases} \quad (2)$$

for proton-neutron collisions. $E$ is the projectile laboratory energy. The coefficients in the above equations have been obtained by a least square fit to the nucleon-nucleon cross section experimental data over a variety of energies, ranging from 10 MeV to 5 GeV.

Most practical studies of medium corrections of nucleon-nucleon scattering are done by considering the effective two-nucleon interaction in infinite nuclear matter, or G-matrix, as a solution of the Bethe-Goldstone equation [10]

$$\langle \mathbf{k}|\mathrm{G}(\mathbf{P},\rho_1,\rho_2)|\mathbf{k}_0\rangle = \langle \mathbf{k}|\mathrm{v}_{NN}|\mathbf{k}_0\rangle - \int \frac{d^3k'}{(2\pi)^3} \frac{\langle \mathbf{k}|\mathrm{v}_{NN}|\mathbf{k}'\rangle Q(\mathbf{k}',\mathbf{P},\rho_1,\rho_2)\langle \mathbf{k}'|\mathrm{G}(\mathbf{P},\rho_1,\rho_2)|\mathbf{k}_0\rangle}{E(\mathbf{P},\mathbf{k}') - E_0 - i\epsilon} \quad (3)$$

with $\mathbf{k}_0$, $\mathbf{k}$, and $\mathbf{k}'$ the initial, final, and intermediate relative momenta of the NN pair, $\mathbf{k} = (\mathbf{k}_1 - \mathbf{k}_2)/2$ and $\mathbf{P} = (\mathbf{k}_1 + \mathbf{k}_2)/2$. Due to energy-momentum conservation, the total momentum, $\mathbf{P}$, remains constant in magnitude and direction, whlile $\mathbf{k}$ remains constant in magnitude. $\mathrm{v}_{NN}$ is the nucleon-nucleon potential. $E$ is the energy of the two-nucleon system, and $E_0$ is the same quantity on-shell. Thus $E(\mathbf{P},\mathbf{k}) = e(\mathbf{P}+\mathbf{k}) + e(\mathbf{P}-\mathbf{k})$, with $e$ the single-particle energy in nuclear matter. It is also implicit in Eq. (3) that the final momenta $\mathbf{k}$ of the NN-pair also lie outside the range of occupied states.

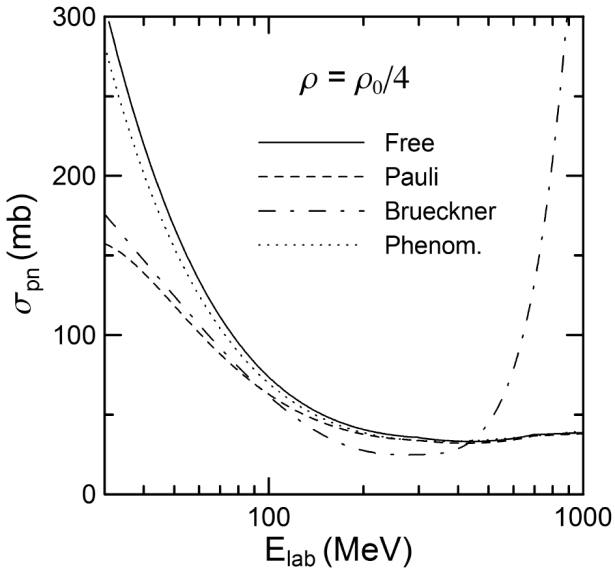


**Figure 1.** Parameterizations of proton-neutron cross sections as a function of the laboratory energy [6]. The solid line is the parametrization of the free $\sigma_{pn}$ cross section given by Eq. (2). The other curves include medium effects for symmetric nuclear matter for $\rho = \rho_0/4$, where $\rho_0 = 0.17$ fm$^{-3}$. The dashed curve includes the geometrical effects of Pauli blocking, as described by Eq. (6). The dashed-dotted curve is the result of the Dirac-Brueckner approach, Eq. (7), and the dotted curve is the phenomenological parametrization, Eq. (8).

Eq. (3) is density-dependent due to the presence of the Pauli projection operator $Q$, defined by

$$Q(\mathbf{k}, \mathbf{P}, \rho_1, \rho_2) = \begin{cases} 1, & \text{if} \quad k_{1,2} > k_{F1,F2} \\ 0, & \text{otherwise.} \end{cases} \tag{4}$$

with $k_{1,2}$ the magnitude of the momenta of each nucleon. $Q$ prevents scattering into occupied intermediate states. The Fermi momenta $k_{F1,F2}$ are related to the proton and neutron densities by means of the zero temperature density approximation, $k_{Fi} = (3\pi^2\rho_i/2)^{1/3}$. For finite nuclei, one usually replaces $\rho_i$ by the local densities to obtain the local Fermi momenta. This is obviously a rough approximation, but very practical and extensively used in the literature. Only by means of several approximations, Eq. (3) can be related to nucleon-nucleon cross sections. If one neglects the medium modifications of the nucleon-mass, and scattering through intermediate states, the medium modification of the NN cross sections can be accounted for by the geometrical factor $Q$ only, that is,

$$\sigma_{NN}(k, \rho_1, \rho_2) = \int \frac{d\sigma_{NN}^{free}}{d\Omega} Q(k, P, \rho_1, \rho_2) d\Omega, \tag{5}$$

where $Q$ is now a simplified geometrical condition on the available scattering angles for the scattering of the NN-pair to unoccupied final states.

The numerical treatment of Pauli corrections is considerably simplified by the assumption of isotropic free-space NN cross sections. In this case, a formula which fits the numerical integration

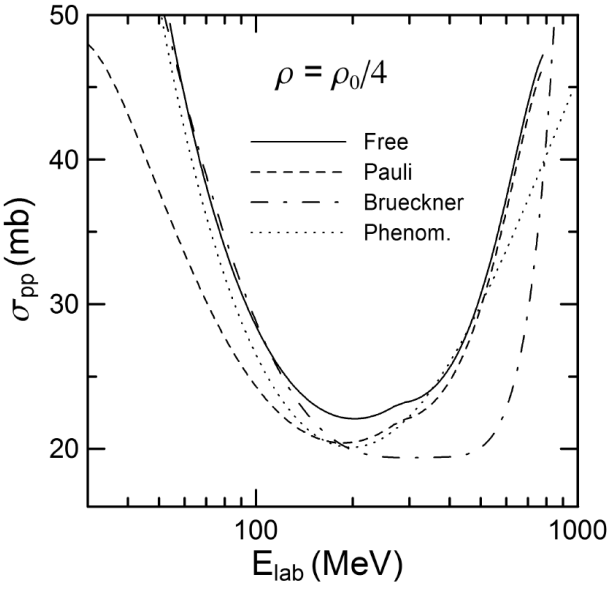


**Figure 2.** Same as in Figure (1), but for pp collisions [6].

of the geometrical model reads [6]

$$\begin{aligned}\sigma_{NN}(E,\rho_p,\rho_t) &= \sigma_{NN}^{free}(E)\frac{1}{1+1.892\left(\frac{2\rho_<}{\rho_0}\right)\left(\frac{|\rho_p-\rho_t|}{\tilde{\rho}\rho_0}\right)^{2.75}} \\ &\times \begin{cases} 1-\dfrac{37.02\tilde{\rho}^{2/3}}{E}, & \text{if } E > 46.27\tilde{\rho}^{2/3} \\ \dfrac{E}{231.38\tilde{\rho}^{2/3}}, & \text{if } E \leq 46.27\tilde{\rho}^{2/3} \end{cases}\end{aligned} \tag{6}$$

where $E$ is the laboratory energy in MeV, $\tilde{\rho} = (\rho_p + \rho_t)/\rho_0$, $\rho_< = \min(\rho_p, \rho_t)$, $\rho_{i=p,t}$ is the local density of nucleus $i$, and $\rho_0 = 0.17$ fm$^{-3}$.

The Brueckner-Hartree-Fock approach to calculate the in-medium scattering amplitude (from which the cross sections are obtained) includes, besides Pauli blocking, the so-called "dispersive effects" which account for the change of the nucleon energy in the presence of the medium. In addition, medium modifications of the NN potential are applied in the Dirac-Brueckner-Hartree-Fock method, but not in the Brueckner-Hartree-Fock method. An example is the work presented in Ref. [11, 12], where a practical parametrization was given, which we will from now on refer as Dirac-Brueckner approach. It reads[1]

$$\begin{aligned}\sigma_{np} &= \left[31.5 + 0.092\left|20.2 - E^{0.53}\right|^{2.9}\right]\frac{1+0.0034E^{1.51}\rho^2}{1+21.55\rho^{1.34}} \\ \sigma_{pp} &= \left[23.5 + 0.00256\left(18.2 - E^{0.5}\right)^{4.0}\right]\frac{1+0.1667E^{1.05}\rho^3}{1+9.704\rho^{1.2}}.\end{aligned} \tag{7}$$

A modification of the above parametrization was done in Ref. [13], which consisted in combining the free nucleon nucleon cross sections parametrized in Ref. [14] with the Dirac-Brueckner

[1] The misprinted factor 0.0256 in Ref. [12] has been corrected to 0.00256.

method results of Ref. [11, 12]. Their parametrization, which tends to reproduce better the nucleus-nucleus reaction cross sections, is

$$\sigma_{np} = \left[-70.67 - 18.18\beta^{-1} + 25.26\beta^{-2} + 113.85\beta\right] \times \frac{1 + 20.88E^{0.04}\rho^{2.02}}{1 + 35.86\rho^{1.9}}$$
$$\sigma_{pp} = \left[13.73 - 15.04\beta^{-1} + 8.76\beta^{-2} + 68.67\beta^{4}\right] \times \frac{1 + 7.772E^{0.06}\rho^{1.48}}{1 + 18.01\rho^{1.46}}, \quad (8)$$

where $\beta = \sqrt{1 - 1/\gamma^2}$ and $\gamma = E[\text{MeV}]/931.5 + 1$. We will denote Eq. (8) as the phenomenological parametrization.

The differences between the parametrization of the Dirac-Brueckner, Eq. (7), the geometrical Pauli blocking, Eq. (6), and the phenomenological one, Eq. (8), are visible. Figure 1 is an example of that, where the varied parameterizations of proton-neutron cross sections are presented as a function of the laboratory energy. The solid line is the parametrization of the free $\sigma_{pn}$ cross section given by Eq. (2). The other curves include medium effects for symmetric nuclear matter for $\rho = \rho_0/4$, where $\rho_0 = 0.17$ fm$^{-3}$. The dashed curve includes the geometrical effects of Pauli blocking, as described by Eq. (6). The dashed-dotted curve is the result of using the Dirac-Brueckner approach, Eq. (7), and the dotted curve is the phenomenological parametrization, Eq. (8). The large departure of results of the Dirac-Brueckner parametrization above 300 MeV is not physical since Eq. (7) is valid only under 300 MeV (pion production threshold) [11, 12]. On the other hand, the differences at lower energies are physical and Pauli-blocking effectively reduces the in-medium *np* cross section. This is not so explicit in the phenomenological parametrization.

The above interpretation cannot be extended to the *pp* cross sections, which are shown in Figure (2). Here it is seen that the geometrical Pauli-blocking correction decreases the cross section much more than in the other cases. Some important differences are also clearly visible at larger energies, $E \gtrsim 100$ MeV/nucleon. We now study the impact of these different methods on direct reactions at intermediate energies.

*2.2. Total reaction cross-sections*

As we mentioned before, obtaining a valid optical potential in knockout reactions [1] and various direct reactions is crucial. One way to test the optical potentials is to reproduce total reaction cross sections. As elastic scattering data at intermediate energies are scarce, for knockout reactions a proper test can be done by calculating total reaction cross sections for the core and the valence particle, separately. The total reaction cross-sections can be obtained in the framework of the eikonal approximation as follows

$$\sigma_R = 2\pi \int db\, b \left[1 - |S(b)|^2\right], \quad (9)$$

where $S$ is the eikonal $S$-matrices. The relation between optical potentials and $S$-matrices is given by

$$S_i(b) = \exp[i\chi(b)] = \exp\left[-\frac{i}{\hbar v}\int_{-\infty}^{\infty} U_{iT}(\mathbf{r})dz\right], \quad (10)$$

where $r = \sqrt{b^2 + z^2}$, and $U_{iT}$ is the particle($i$)-target($T$) optical potential. A semiclassical probabilistic approach has been followed to calculate the cross sections and other observables in direct reactions as described in Refs. [15, 16], and a relation has been established between the optical potential and the nucleon-nucleon scattering amplitude in Ref. [1]. This relation is frequently mentioned in the literature as the "t-$\rho\rho$ approximation". "Experimentally deduced" optical potentials are often not available from elastic and inelastic scattering involving

radioactive nuclei. Therefore, the t-$\rho\rho$ approximation is one of the most practical techniques to obtain optical potentials. In this approximation, the eikonal phase becomes

$$\chi(b) = \frac{1}{k_{NN}} \int_0^\infty dq\ q\ \rho_p(q)\, \rho_t(q)\, f_{NN}(q)\, J_0(qb)\ , \tag{11}$$

where $\rho_{p,t}(q)$ is the Fourier transform of the nuclear densities of the projectile and target, and $f_{NN}(q)$ is the high-energy nucleon-nucleon scattering amplitude at forward angles, which can be parametrized as

$$f_{NN}(q) = \frac{k_{NN}}{4\pi} \sigma_{NN} (i + \alpha_{NN}) \exp\left(-\beta_{NN} q^2\right)\ . \tag{12}$$

One often neglects nuclear medium effects in the experimental analysis of knockout reactions, as pointed out in Ref. [6]. However, their importance has been well known for a long time in the study of elastic and inelastic scattering, as well as of total reaction cross sections [1, 2]. In these situations, a systematic analysis of the medium effects has been presented in Ref. [1], and it has shown that the effects becomes larger at lower energies, where Pauli blocking strongly reduces the nucleon-nucleon cross sections in the medium.

The p + $^{12}$C total reaction cross sections in the energy range of 20-100 MeV/nucleon shown in Figure 3 presents the justification of these statements, where the experimental data taken from the Ref. [17]. The cross sections were calculated from the Eqs. (10,11,12) and $^{12}$C density from a Hartree-Fock-Bogoliubov calculation (HFB) [18]. Various different calculations are shown in Figure 3. The result of Eq. (11) with the free nucleon-nucleon cross sections and the carbon matter density from a HFB calculation [19] is represented by the solid curve, whereas the triangle-dotted curve (the triangles are not data, but used for better visibility) uses a different HFB density [18], consistent with the calculations presented in Ref. [4]. As expected, that the agreement between the two calculations is very good.

The same calculation procedure, but this time including medium corrections for the nucleon-nucleon cross section, has been performed to obtain the other curves in Figure 3. It is

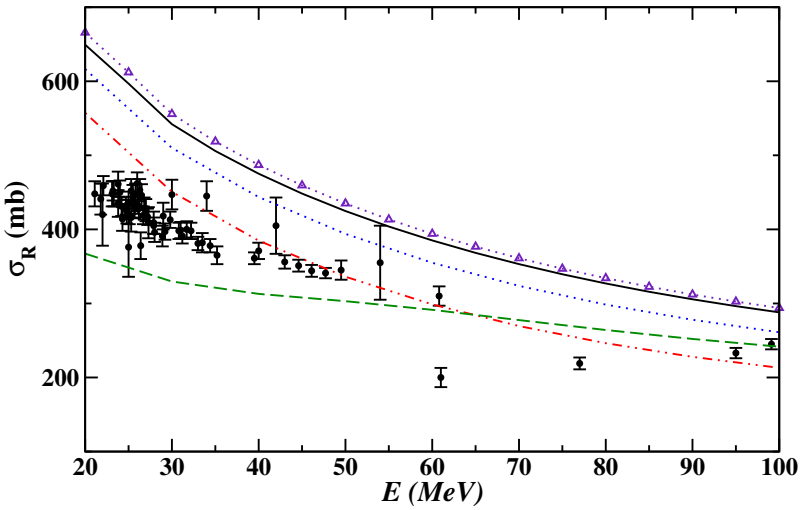


**Figure 3.** The total reaction cross section of the p + $^{12}$C taken from Ref. [17]. The curves are calculated with the free NN cross sections from Ref. [8] (solid), with a geometrical account of Pauli blocking (dashed), a phenomenological fit from Ref. [13] (dotted), and a correction from the Dirac Brueckner approach (dashed-dotted). The triangle-dotted curve is calculated with the same free NN cross sections as in Ref. [8], but with an another HFB calculation [18] for the $^{12}$C ground state density.

evident that the results are very different than the former. The medium effects with various different are shown with the dotted, dashed-dotted, and dashed curves, which they correspond to the calculations with phenomenological, Dirac-Brueckner, and Pauli geometrical methods, respectively. Obviously, medium effects modify the results, yielding a closer reproduction of the data. But the large experimental error bars do not allow a fair judgment of which model reproduces better the data.

*2.3. Nucleon knockout reactions*

Momentum distributions of the projectile-like residues in one-nucleon knockout are a measure of the spatial extent of the wavefunction of the struck nucleon, while the cross section for the nucleon removal scales with the occupation amplitude, or probability (spectroscopic factor), for the given single-particle configuration in the projectile ground state. The longitudinal momentum distributions are given by (see, e.g., Refs. [16, 20, 21])

$$\frac{d\sigma_{\rm str}}{dk_z} = (C^2S)\frac{1}{2\pi}\frac{1}{2l+1}\sum_m \int_0^\infty d^2b_n \left[1-\left|S_n\left(b_n\right)\right|^2\right] \times \int_0^\infty d^2b_c \ \left|S_c\left(b_c\right)\right|^2 \left|\int_{-\infty}^{\infty} dz \exp\left[-ik_z z\right]\psi_{lm}\left(\mathbf{r}\right)\right|^2 , \quad (13)$$

where $k_z$ represents the longitudinal component of $\mathbf{k}_c$ (final momentum of the core of the projectile nucleus) and $(C^2S)$ is the spectroscopic factor, and $\psi_{lm}\left(\mathbf{r}\right)$ is the wavefunction of the core plus (valence) nucleon system $(c+n)$ in a state with single-particle angular momentum $l, m$.

*2.3.1.* $^{12}$C($^{17}$C,$^{16}$B)X *at* 35 MeV/u

The one-proton removal reaction, $^{12}$C($^{17}$C,$^{16}$B)X, from $^{17}$C at 35 MeV/nucleon has been measured with the aim to explore the low-lying structure of the unbound $^{16}$B nucleus. In Ref. [22], the unbound $^{16}$B nucleus is assumed to be a $d$-wave neutron decay from $^{15}$B+$n$ system. Here, we have focused to study the consequences of medium corrections on the transverse

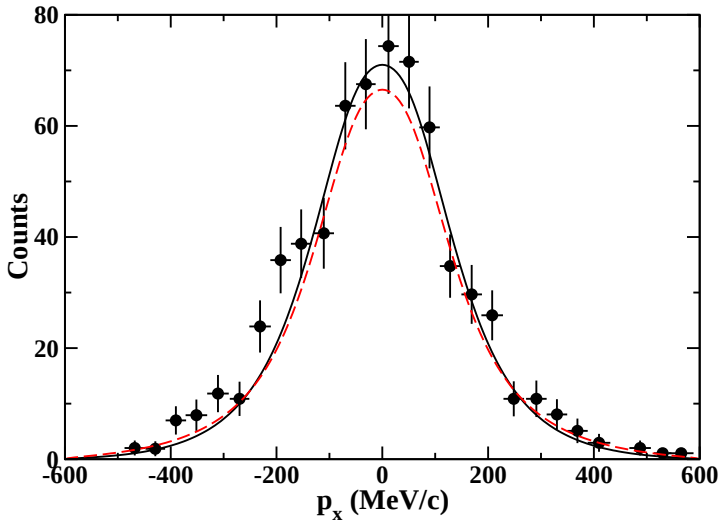


**Figure 4.** Transverse momentum distributions for the $^{12}$C($^{17}$C,$^{16}$B)X system at 35 MeV/u. Solid lines represent calculations including medium corrections. Dashed lines stem from calculations that do not include medium corrections. The data are taken from Ref. [22].

momentum distribution of the $^{16}$B fragment following the same assumptions as in Ref. [22]. The configuration mixing of the proton removed from $^{17}$C is assumed to be

$$\begin{aligned} |^{17}\mathrm{C}\rangle &= \alpha_1|^{16}\mathrm{B}(0^-)\otimes\pi 1p_{3/2}\rangle \\ + \quad &\alpha_2|^{16}\mathrm{B}(3_1^-)\otimes\pi 1p_{3/2}\rangle + \alpha_3|^{16}\mathrm{B}(2_1^-)\otimes\pi 1p_{3/2}\rangle \\ + \quad &\alpha_4|^{16}\mathrm{B}(2_2^-)\otimes\pi 1p_{3/2}\rangle + \alpha_5|^{16}\mathrm{B}(1_1^-)\otimes\pi 1p_{3/2}\rangle \\ + \quad &\alpha_6|^{16}\mathrm{B}(3_2^-)\otimes\pi 1p_{3/2}\rangle, \end{aligned} \tag{14}$$

where $\alpha_i$ is the spectroscopic amplitude for a core-single particle configuration $i = (c \otimes nlj)$.

In Ref. [22] a good agreement between data and calculated transverse momentum distributions was achieved using the spectroscopic factors from a shell-model calculation with the WBP interaction [23]. However, they have obtained a theoretical result of 24.7 mb for total cross section which diverges from the measured cross-section, 6.5(1.5) mb. In Ref. [24], an explanation is proposed to this large discrepancy as due to a reduction of the spectroscopic factor by 70% for strongly bound nucleon systems. The theoretical estimates for the cross section with the reduction at the spectroscopic factor becomes 7.5 mb, in reasonable accordance with the data. We do not challenge the assumptions of Ref. [22], and we use the same configuration mixing and spectroscopic factors as in [22]. The proton binding potential parameters are given in Ref. [7], which are adjusted to obtain the effective separation energies. Here, as it is shown in Figure 4, we find that medium corrections change the cross sections by 5% which is rather small to explain the observed difference with the total cross sections.

*2.3.2.* $^{9}$Be($^{11}$Be,$^{10}$Be)X *at* 60 MeV/u

In order to further understand the medium effects on knockout reactions, we consider the $^{9}$Be($^{11}$Be,$^{10}$Be)X system at 60 MeV/u which can be modeled by a core plus valence system with the assumption $^{10}\mathrm{Be}_{gs}(0^+)$ + n in $2s_{1/2}$ orbital for the ground state of $^{11}\mathrm{Be}_{gs}(1/2^+)$ ($S_n = 0.504$ MeV). Here we use the same Woods-Saxon potential parameters for the bound state as published in Ref. [16]: ($R_0 = 2.70$ fm, $a_0 = 0.52$ fm). In Figure 5 and Table 1 we present our results for the the neutron removal longitudinal momentum distribution of 60 MeV/nucleon

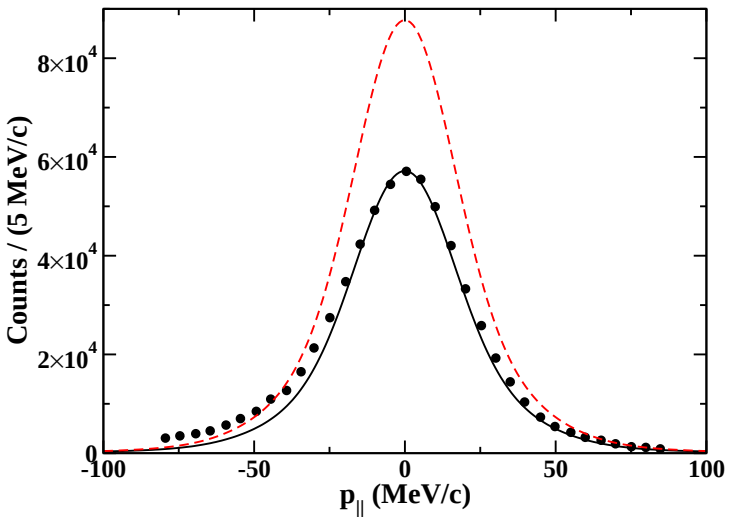


**Figure 5.** Longitudinal momentum distributions of for the reaction $^{9}$Be($^{11}$Be,$^{10}$Be) at 60 MeV/nucleon. Solid lines represent calculations including medium corrections. Dashed lines stem from calculations that do not include medium corrections. The data is taken from Ref. [25].

$^{11}$Be projectiles incident on $^{9}$Be targets. We find that medium corrections for this system change the cross sections by 50% which is quite big.

It has been show that $^{17}$C has a small "effective" size and that $^{11}$Be has a large effective size among the low energy systems studied in Ref. [7]. Therefore, the wavefunctions of weakly bound systems extend far within the target where the nucleon-nucleon cross sections are strongly modified by the medium. Momentum distributions and nucleon removal cross sections in knockout reactions are thus expected to change appreciably with the inclusion of medium corrections of nucleon-nucleon cross section. Such corrections are also expected to play a more significant role for loosely-bound systems.

| $\sigma_{-1n}$ | $^{12}$C($^{17}$C,$^{16}$B) | | $^{9}$Be($^{11}$Be,$^{10}$Be) | |
|---|---|---|---|---|
| $= \sigma_{dif} + \sigma_{str}$ | Full | no medium | Full | no medium |
| Strip. [mb] | 7.56 | 5.63 | 122.5 | 164.1 |
| Diff. [mb] | 18.42 | 19.15 | 49.6 | 97.3 |
| Total [mb] | 25.98 | 24.78 | 172.1 | 261.4 |

**Table 1.** The cross sections calculated for the systems, $^{12}$C($^{17}$C,$^{16}$B) at 35 MeV/nucleon and $^{9}$Be($^{11}$Be,$^{10}$Be) at 60 MeV/nucleon.

## 3. Summary

In this small report, we have explored the importance of the medium modifications of the nucleon-nucleon cross sections on direct reactions, and particularly on knockout reactions. It has been shown that the effects are noticeable at low energies. Nonetheless, we have noticed that medium effects do not lead to sizable modifications on the shapes of momentum distributions. We have shown this explicitly by comparing our results with a large number of available experimental data in Ref. [7]. As expected on physics grounds, these corrections are larger for experiments at lower energies, around 50 MeV/nucleon, and for weakly bound nuclei.

Medium effects in knockout reactions have been frequently ignored in the past. We have shown that they have to be included in order to obtain a better accuracy of the extracted spectroscopic factors. Although these conclusions might not come as a big surprise, they have not been properly included in many previous experimental analyses.

## Acknowledgments

This work was partially supported by the US-DOE grants DE-SC004972 and DE-FG02-08ER41533 and DE-FG02-10ER41706, and by the Research Corporation.

## 4. References

[1] Hussein M, Rego R, and Bertulani C A 1991 *Phys. Rep.* **201** 279
[2] Ray L 1979 *Phys. Rev. C* **20** 1857
[3] Trache L, Carstoiu F, Gagliardi C A, and Tribble R E 2001 *Phys. Rev. Lett.* **87** 271102
[4] Trache L, Carstoiu F, Mukhamedzhanov A M, and Tribble R E 2002 *Phys. Rev. C* **66** 035801
[5] Bertulani C A 2001 *J. Phys. G* **27** L67
[6] Bertulani C A, and De Conti C 2010 *Phys. Rev. C* **81** 064603
[7] Karakoc M, Banu A, Bertulani C A, and Trache L arXiv:1201.3677.
[8] John S, Townsend L W, Wilson J W, and Tripathi R K 1993 *Phys. Rev. C* **48** 766
[9] Particle Data Group 2006 *J. Phys. G* **33** 1
[10] Gomes L C, Walecka J D, and Weisskopf V F 1958 *Ann. Phys. (N.Y.)* **3** 241
[11] Li G Q, and Machleidt R 1993 *Phys. Rev. C* **48** 1702
[12] Li G Q, and Machleidt R 1994 *Phys. Rev. C* **49** 566
[13] Xiangzhou C, Jun F, Wenqing S, Yugang Ma, Jiansong W, and Wei Ye 1998 *Phys. Rev. C* **58** 572

[14] Charagi S K, and Gupta S K 1990 *Phys. Rev. C* **41** 1610
[15] Hussein M S, McVoy K W 1985 *Nucl. Phys. A* **445** 124
[16] Hencken K, Bertsch G, and Esbensen H 1996 *Phys. Rev. C* **54** 3043
[17] Carlson R F 1996 *At. Data Nucl. Data Tables* **63** 93
[18] Beiner M, and Lombard R J 1974 *Ann. Phys. (N.Y.)* **86** 262;
Carstoiu F and Lombard R J 1992 *ibid.* **217** 279
[19] http://www.nscl.msu.edu/ brown/resources/resources.html
[20] Bertulani C A, and Hansen P G 2004 *Phys. Rev. C* **70** 034609
[21] Bertulani C A, and Gade A 2006 *Comp. Phys. Comm.* **175** 372
[22] Lecouey J L et al. 2009 Phys. Lett. B **672** 6
[23] Warburton E K, and Brown B A 1992 *Phys. Rev. C* **46** 923
[24] Gade A et al. 2004 *Phys. Rev. Lett.* **93** 042501
[25] Aumann T et al. 2000 *Phys. Rev. Lett.* **84** 35